

LABORATORY INVESTIGATION OF THE FORMATION OF STABLE  
CANAL CHANNELS

N. A. Mikhailova, O. B. Shevchenko, and M. M. Selyametov

UDC 556.535.6

Canals designed on the basis of the existing technical specifications and standards are rather often subjected to considerable deformations during operation. One of the main problems when designing an artificial watercourse is to create a stable (nondeformable) channel of maximum capacity at a minimum cost (including operating costs).

When calculating the cross section of canals in erodible soil the values of the average velocity and depth of the flow are usually used and the differences in the character of deformation (removal of particles) of the slopes and bottom of the canals are disregarded.

The main purpose of the present investigations was to establish the regularities of the formation of dynamically stable canal channels. By dynamically stable we will mean a channel in which the average parameters of the channel do not change with time despite the longitudinal transport of sediments and migration of channel bed forms. In this case it is considered that averaging is done during a time determined by the rate of migration of characteristic bed forms [1].

The experiments were conducted on a channel flume of the hydrophysical laboratory of the Department of Physics of the Sea and Land Waters, Moscow State University. The flume had the following dimensions: length 24 m, width 4 m, wall height 1 m. The flume has a carriage for installing instruments, which can move along the flume. Water discharge was determined by means of a trapezoidal weir installed in the head part of the flume. The slope of the bottom and free surface of the flow was measured by a point gauge. The following apparatus was used for determining the velocity characteristics: for measuring the average velocities, an impact-pressure tube; for recording the fluctuation velocity modulus, a spring vane with a photoelectric attachment; for recording the fluctuation horizontal and vertical components of the velocity, a wire angular thermohydrometer with a platinum filament. The velocity fluctuations during measurement by the vane were recorded on an N-373-2 recorder and during measurement by the angular thermohydrometer on the high-speed N-327-3 recorder.

Three series of experiments were conducted on erodible models of various cross sections made of natural Amu Darya sand,  $d_{av} = 0.2$  mm (Table 1). In experiment 1 the initial average velocity of the flow  $u$  was assigned from the condition  $u > u_0$ , where  $u_0$  is the noneroding velocity. In experiment 2 with the same trapezoidal cross section of the canal the initial av-

TABLE 1

Experi- ment	Time from start of expt.	Discharge $Q$ , liters/ sec	Av. depth $h_{av}$ , cm	Max. depth $h_{max}$ , cm	Width at water edge $B$ , cm	Side slopes, m	Slope of water surface $1 \cdot 10^3$	Av. ve- locity $u$ , cm/sec	Max. ve- locity $u_{max}$ , cm/sec	Cross- sectional area $\omega$ , cm <sup>2</sup>	$\frac{B}{h_{av}}$	$\frac{B}{h_{max}}$
1	0	65,0	14,2	19,5	143	2	2,0	32,0	56,8	2028	9,8	6,9
	59 h 05 min	65,0	8,2	10,4	223		2,0	35,6	43,1	1824	27,2	24,1
	114 h 10 "	65,0	6,9	10,4	362		1,8	25,9	33,9	2505	52,4	34,8
2	0	44,0	14,3	19,6	143	2	1,0	21,5	34,4	2042	10,0	7,3
	27 h 55 min	47,0	8,4	13,2	161		1,0	32,5	35,2	1354	19,2	12,2
	51 h 40 "	47,0	9,9	14,0	170		1,0	26,2	29,1	1676	17,2	12,1
	113 h 55 "	47,0	9,2	13,1	193		1,0	24,9	39,0	1768	21,0	14,7
3	0	69,0	17,7	27,2	137	Cosine curve	0,5	28,5	—	2423	7,7	5,0
	3 h 30 min	69,0	14,8	27,6	146		0,6	32,9	35,7	2096	11,9	5,3
	78 h	69,0	10,7	16,0	216		0,7	29,8	35,7	2312	20,2	13,5
	217 h	69,0	10,0	14,4	265		0,8	26,0	30,3	2655	26,5	13,4

Translated from *Gidrotekhnicheskoe Stroitel'stvo*, No. 7, pp. 41-46, July, 1980.

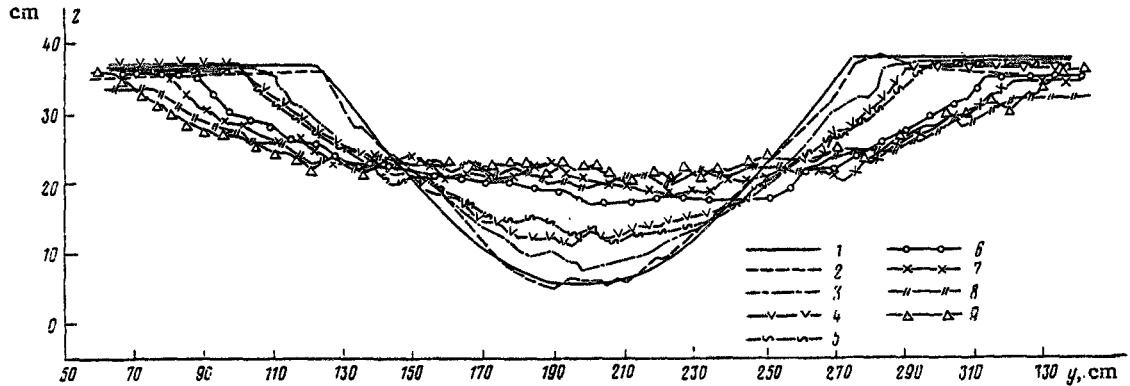


Fig. 1. Transverse profiles of the canal. 1-9) Respectively, before the experiment and 6, 26, 40, 47, 89, 159, and 187 h after the start of the experiment.

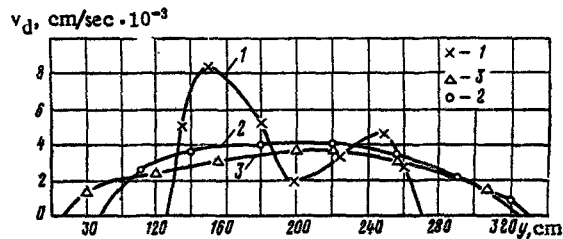


Fig. 2. Distribution of the propagation rate of dunes 1-3 over the width of the channel 2, 78, and 217h from the start of the experiment.

erage velocity due to a decrease of slope was less than the noneroding, i.e., the condition  $u < u_0$  was fulfilled. In experiment 3 with a discharge close to the value of the discharge in experiment 1 the hydraulic elements of the model were determined from the value of the critical tractive force [2]. For  $d_{av} = 0.2$  mm the critical tractive force was equal to  $[\tau] = 0.0132$  MPa, and the angle of repose was equal to  $\varphi = 32^\circ$ . The initial average velocity in experiment 3 was practically equal to the noneroding  $u = u_0$ . The cross section of the canal in experiment 3 had the form of a cosine curve. The duration of each experiment was determined by the composition of the measurements and condition of formation of a dynamically stable canal cross section.

At the initial time of formation of the channel, regardless of the form of its cross section, channel deformation has mainly the same character. Originally the crests of the subaqueous dunes formed near the water edge form an acute angle with it. In this case the canal bottom remains practically stationary.

Movement of the sand dunes causes intense deformation of the slope, in which case the region occupied by the dunes enlarges. The direction of the dune crest is preserved with respect to the water edge. The dunes move parallel to one another. Movement of the sand grains toward the axis of the flow is observed in the trough of the dunes. Dunes begin to form also on the canal bottom from the grains that rolled down the slopes, which, unlike the dunes on the slope, are perpendicular to the axis of the flow. From the time of formation of dunes on the canal bottom the rate of movement of the particles here increases markedly. Particles moving from the slope are added to the particles detached from the canal bottom. As a consequence of this the total amount of sand brought into motion exceeds the transporting capacity of the flow, which leads to deposition of sediments on the bottom in an amount determined by the difference between the sediment discharge and transporting capacity of the flow. This leads to an increase of the level of the bottom. At this time intense erosion of the slopes begins, leading to widening of the channel.

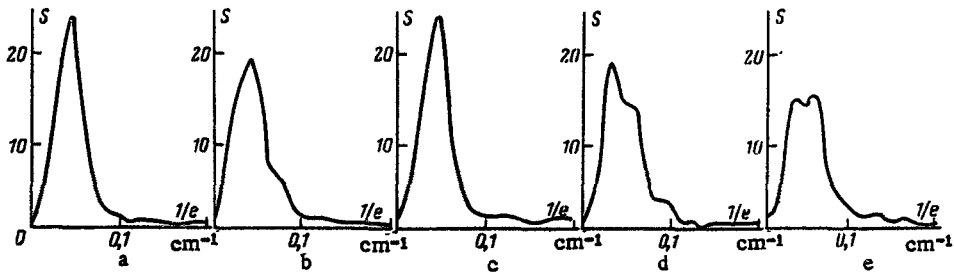


Fig. 3. Spectral functions of the elevations of the relief in the longitudinal section along the axis of the canal from the start of experiment (a, b, c, d, and e are, respectively, 31, 40, 88, 127, and 152 h from the start of the experiment).

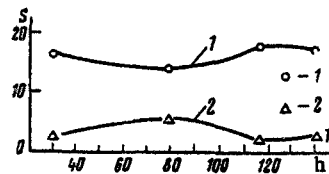


Fig. 4. Change in the spectral density of the elevations of the relief at characteristic "frequencies" with time.

During each experiment measurements were systematically taken of the level of the bottom on various verticals of the investigated cross section. Some of the profiles obtained for experiment 3 are shown in Fig. 1.

For various stages of channel formation Fig. 2 shows the distribution of the propagation rate of sand dunes over the width of the flow, which is an important characteristic of the intensity of the channel-forming process. The distance from the right wall of the flume is plotted on the  $x$  axis (the axis of the flow corresponds to elevation  $y = 200$  cm). In the initial stage of formation of the canal channel the propagation rate of the dunes (and consequently the specific sediment discharge) on its slopes is considerably greater than on the bottom, where the dunes begin to form later. Curve 1 in Fig. 2, plotted from the data of measurements 2 h after the start of experiment 3, corresponds to this case.

Correlation and spectral analysis were used for determining the character of the change in the characteristics of the relief during transition from the initial to stable canal section. The elevations of the relief were recorded at various stages of channel formation along longitudinal sections parallel to the axis of the flow with a 2.5-cm spacing. The normalized correlation function was determined by the expression

$$r(a) = \frac{\overline{z'(x)z'(x+a)}}{\overline{z'^2}}$$

where  $z'$  is the deviation from the average (moving average with a Tukey cosine-nucleus) values of the elevations of the relief,  $\overline{z'^2}$  is the variance of the elevations of the relief (the horizontal bar denotes probability averaging). The spectral function was calculated from the correlation function by inverse Fourier transformation

$$S(k) = 4 \int_0^{\infty} r(a) w(a) \cos 2\pi k a d\tau,$$

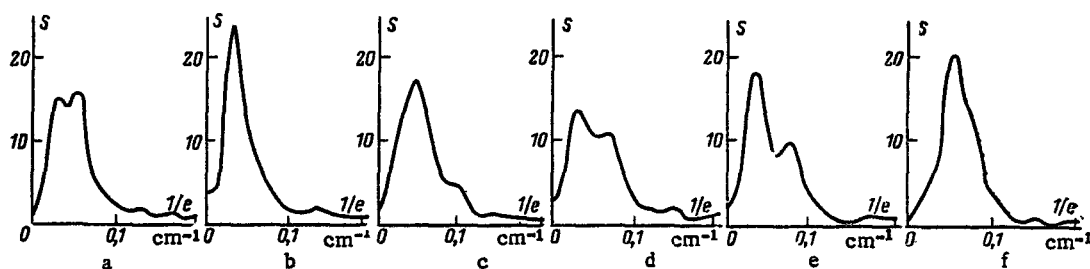


Fig. 5. Spectral functions of elevations of the relief in longitudinal sections at various distances from the axis of the flow in the presence of a stable canal section in experiment 3 (a, b, c, d, e, and f:  $y = 200, 240, 260, 280, 300,$  and  $320$  cm).

where  $k$  is the conditional "frequency" (number of waves per unit length);  $a$ , the distance along the flow;  $w(a)$  the Tukey spectral window [4]. The statistical processing program used is described in [5]. The lengths of the realizations and the discreteness spacing made it possible to reveal the presence on the bottom of sand waves whose lengths varied from 5 to 150 cm.

Figure 3 shows the spectral functions of the elevations of the relief in the longitudinal section along the canal axis (transverse coordinate  $y = 200$  cm) 31, 40, 88, 127, and 152 h after the start of experiment 3. The quantity  $k$ , characterizing the number of waves per unit length ("frequency"), is plotted on the x axis. In the initial stage of formation of the channel, when on the bottom there are small dunes differing little from one another in size, the spectra are unimodal. With the course of time these dunes grow, and the characteristic "frequency" to which corresponds the maximum value of the spectral density function, decreases. Complication of the relief occurs gradually; larger structural formations appear along with the existing dunes. As a consequence of this the form of the spectra becomes complicated, additional peaks appear on them at "frequencies" corresponding to large bed forms, which are determining in the formed channel. The width of the spectral curves for a given value of the spectral density function characterizes the degree of concentration of the thickness of the structural formations at the characteristic "frequency." In the formed channel the spectra are more wide-band. An analysis of the spectral curves of the elevations of the relief for the various experiments showed that in the presence of bimodal curves a multiplicity of the characteristic "frequencies" is observed in the majority of cases. For each of them the value of the spectral density varies with the course of time. Figure 4 illustrates this circumstance for one of the longitudinal sections in experiment 3 ( $y = 260$  cm). The change in the spectral density of the first 1 and second 2 peaks occurs in opposite phase.

The characteristics of the bottom relief vary over the width of the channel, which is indicated by the spectral characteristics of the elevations of the relief in longitudinal sections at various distances from the axis of the flow in the presence of a stable canal section shown in Fig. 5.

To find a relation between the characteristics of the flow (geometric and kinematic) and parameters of the dunes, we investigated the change during formation of a stable canal section in the dimensionless parameter  $C = (\sqrt{gh}/L)(l/u)$ , where  $l$  is the characteristic dimension of the dunes determined from the spectrum of the elevations of the relief in the axial section of the canal;  $L$ , length of the canal;  $h$ , depth;  $u$ , vertically average velocity on the canal axis. The indicated graph for the results of experiment 3 is shown in Fig. 6 for an example. In selecting the dimensionless parameter we took for the basis the results of investigations indicating a relation between the dimensions of the bed forms and the dimensions of ordered structural formations in the flow and dependence of the dimensions of these formations on the geometric and kinematic characteristics of the flow. The following relation is proposed for the characteristic frequency of velocity fluctuations

$$f_n = \frac{1}{2L} (u + n\sqrt{gh}). \quad (1)$$

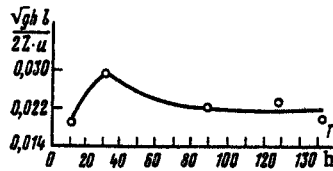


Fig. 6. Change in the dimensionless parameter  $(\sqrt{gh}/2L)(l/u)$  with time.

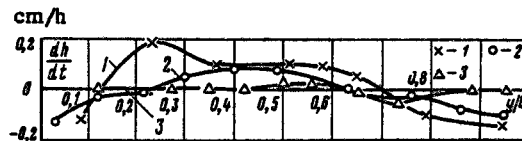


Fig. 7. Change in the rate of deformation of the cross section of the canal 1-3 over its width in experiment 3, respectively, 0, 85, and 187 h from the start of the experiment.

where  $n$  is the number of the harmonic. Considering that the dimensions of the bed forms are determined by the fluctuation characteristics of the velocity, which depend on the geometric (longitudinal) dimensions and average velocity of the flow, we took as the basis the give relation also for calculating the characteristic "frequency" of bed forms. In the investigated case the second term is considerably greater than the first. Therefore, the relation  $\sqrt{gh}/L$ , which was normalized to the quantity  $u/L$ , was taken as the measure of the characteristic frequencies of velocity fluctuations.

As a quantitative estimate of the intensity of channel deformations on each vertical of the investigated cross section we used the quantity  $dh/dt$ , which was determined in the following way. On the basis of the data obtained the time dependence of the change in the elevations of the canal bed  $\Sigma\Delta h_i = f(t)$  was investigated for certain verticals spaced 20 cm apart. The quantity  $\Sigma\Delta h_i$  was determined as the difference between the original elevation of the bottom on the investigated vertical and the elevation of the bottom at the time of measurement. The plus sign corresponds to deposition and the minus sign to erosion. The indicated calculations were made for the initial, intermediate, and final times. The approximate value of the derivative was determined as  $dh/dt \approx \Delta h/\Delta t$ . The value of  $\Delta t$  was assumed equal to 4 h, the value of  $\Delta h$  was equal to the difference of elevations of the bottom during time interval  $\Delta t$ . One such graph clearly illustrating the process of formation of a stable canal cross section is shown in Fig. 7. At the initial time in all experiments  $dh/dt$  differed substantially from zero. In the middle part of the channel this quantity has a positive value, which decreases from the middle of the channel toward the banks. At a certain distance from the bank  $dh/dt$  "passes" through zero and takes on maximum negative values in the near-edge zone.

During formation of the canal there occurs a decrease in the flow velocity over the entire section, a decrease of the velocity gradient in the bank region, and an increase of the standard deviation of the average velocity over the entire section. Figure 8 shows the distribution of the average velocity and standard deviation in the canal section at various stages of its formation in experiment 2 (at the bottom, over the depth of the flow on various verticals; at the top, across the flow, of depth-averaged values). The distribution over the flow width of the Froude number  $Fr$  at various stages of formation of the channel was determined from the data obtained (Fig. 9). A comparison of the curves pertaining to various stages of erosion shows that at the initial time a narrow region of increased  $Fr$  values exists in canals near the bank. The dimensions of this region coincide with the dimensions of the stretch of the section subjected to erosion, i.e., it is equal to the distance from the water edge to the vertical where the rate of deformations takes on a zero value (Fig. 7).

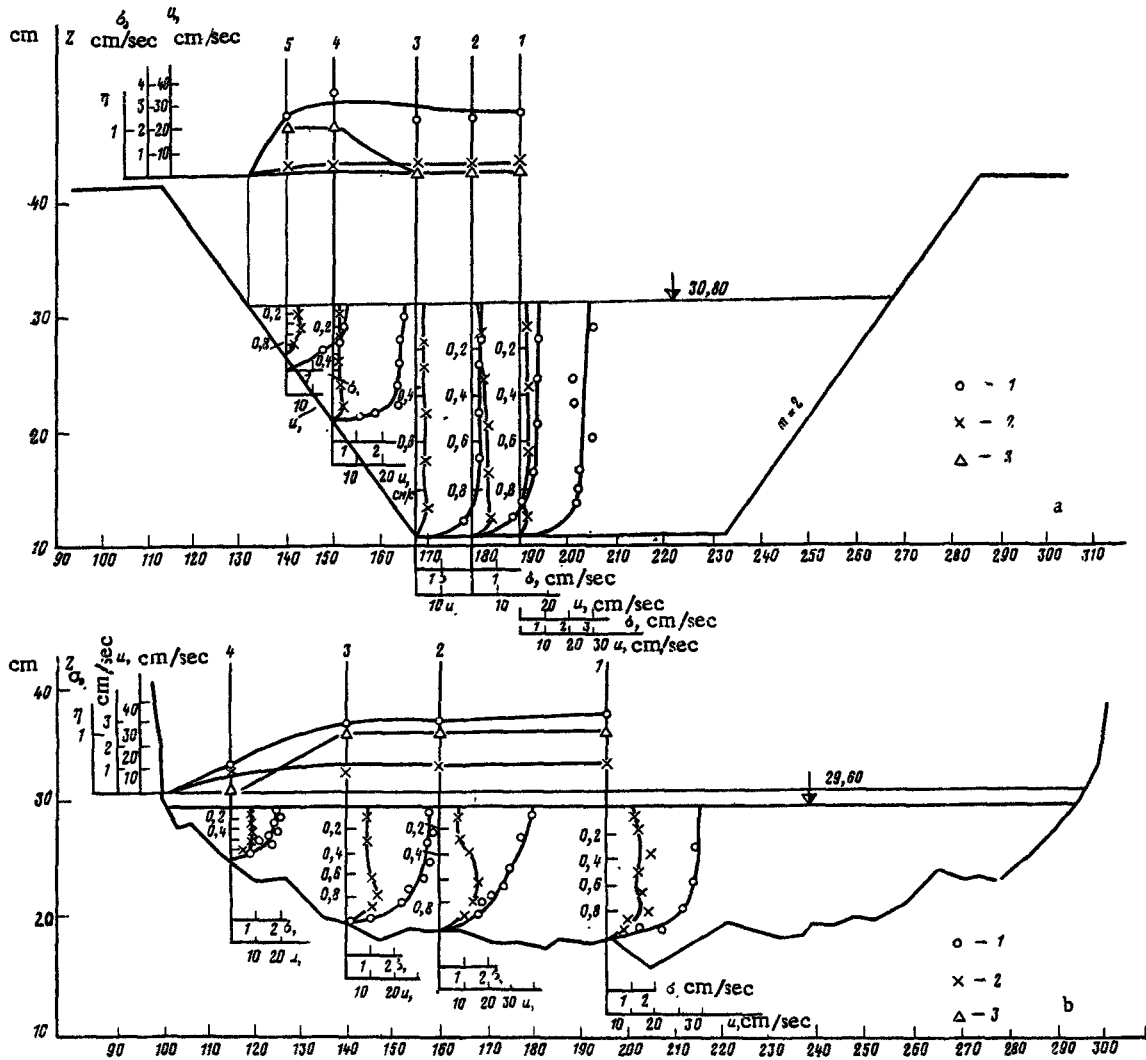


Fig. 8. Distribution in the canal section of the average velocity 1 and standard deviation 2 (at the bottom, over the depth of the flow on various verticals; at the top, across the flow, of depth-averaged values) in experiment 2 at different stages of channel development. a) Start of experiment; b) 114 h after the start of the experiment. At the top is the probability of the removal of solid particles (3).

One of the problems of these investigations was to compare the values of the shear stresses, determined by a simplified formula applicable for practical calculations

$$\tau_c = \gamma h I \tag{2}$$

where  $\gamma$  is the specific weight of the fluid,  $h$  is the depth of the flow,  $I$  is the slope of the water surface, with the actual values of the shear stress obtained as a result of direct measurements. To determine the shear stress we used recordings of two velocity components by the angular thermohydrometer [3] with a platinum filament. The value of  $\tau$  was determined by the formula

$$\tau = -\rho \overline{|u'v'|}, \tag{3}$$

where  $\rho$  is the density of the fluid;  $u'$  and  $v'$  are, respectively, the fluctuations of the instantaneous values of the horizontal and vertical velocity components. In the initial stage of channel formation the shear stress in the bottom region  $\tau = 0.033$  MPa exceeds the deter-

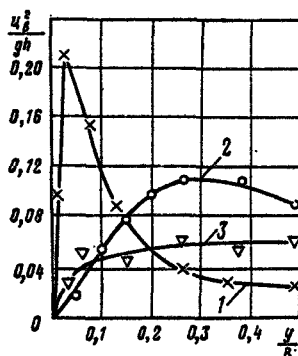


Fig. 9. Distribution of the Froude number in the canal cross section, experiment 2. 1-3) Respectively, the start of the experiment and 52 and 114 h after the start of the experiment.

mination by Eq. (2) and is equal to  $\tau_c = 0.0118$  MPa. In the formed stable channel the distribution of shear stress over the depth of the flow is more uniform, but its value in the bottom region  $\tau = 0.008$  MPa is less than the value calculated by Eq. (2)  $\tau_c = 0.0105$  MPa. Thus, the experimental data obtained show that the approximate relation (2) cannot be used for calculating the shear stress in flows with a three-dimensional kinematic structure.

An analysis of the experimental data obtained shows that calculations with respect to the permissible tractive force or eroding velocity do not make it possible to construct a canal with a cross section which would not be deformed. Thus, during formation of a stable section the canal calculated with respect to the noneroding velocity (experiment 1) widened by a factor of 2.5, at a velocity 22% less than the noneroding (experiment 2) by a factor of 1.4, and the canal calculated with respect to the permissible tractive force (experiment 3) by a factor of 1.9 (Table 1).

The instantaneous velocity  $u$  can be greater or less than the mean velocity  $\bar{u}$ . Therefore, even in the case when the critical velocity exceeds the mean velocity, i.e.,

$$u_0 > \bar{u}, \quad (4)$$

a situation satisfying the condition

$$u > u_0, \quad (5)$$

can arise and solid particles will be removed.

According to the Einstein-Velikanov theory [1], the probability of the removal of a solid particle from the bottom of a flow, on the assumption of the validity of a normal distribution of the instantaneous velocity values, will be equal to

$$\eta = \frac{1}{\sqrt{2\pi}\sigma_u} \int_{u_0}^{\infty} e^{-\frac{(u-\bar{u})^2}{2\sigma_u^2}} du, \quad (6)$$

where  $\bar{u}$  is the mean velocity;  $u$ , instantaneous velocity;  $\sigma_u$ , standard deviation from the average value of the velocity;  $u_0$ , critical velocity at which the gravitational force is balanced by the lifting force. Here, generally speaking, reference is to the kinematic characteristics of the flow in the bottom region. But since there is a relation between the characteristics of the flow in the bottom region and the depth-averaged characteristics, we will henceforth keep in mind the latter (allowing certain inaccuracies in this case).

For a given distribution of the instantaneous velocity values, the probability of deformation of the bottom will be determined in relation to how much the instantaneous velocity

of the flow exceeds the mean. The preceding expression confirms that a nonzero value of  $\eta$  is obtained when  $u_0 > \bar{u}$ . In the case of a normal distribution of the instantaneous velocity values a nonzero probability of removal of particles will occur if

$$\bar{u} + 3\sigma_u > u_0. \quad (7)$$

Expression (6) can be transformed to the form

$$\eta = (1/2) \pm \Phi(\mu), \quad (8)$$

where

$$\mu = \frac{u_0 - \bar{u}}{\sigma_u};$$

$$\Phi(\mu) = \frac{1}{\sqrt{2\pi}} \int_0^{\mu} e^{-z^2} dz; \quad z = \frac{u - \bar{u}}{\sigma_u}. \quad (9)$$

The choice of the sign in Eq. (8) is determined by the condition: plus when  $\mu < 0$  and minus when  $\mu > 0$ .

In the present work an attempt was made to use the probability theory of movement of the bed load for the case of a three-dimensional flow. We will consider that in this case the general considerations that the probability of deformation of the canal cross section determined by the value of parameter  $\mu$  calculated from the characteristics of a particular vertical in the investigated section are valid. The numerator in Eq. (9) characterizes the excess of the mean velocity over the critical, and the denominator is equal to the standard deviation of the instantaneous velocity values from the mean. Owing to the complexity of a theoretical determination of the critical velocity, for its calculation we used the empirical relation

$$u_0 = 0.64 \sqrt{hd}, \quad (10)$$

where  $h$  is the depth, m;  $d$ , the diameter of the particles, mm.

We will assume that the probability of removal of a particle from the bottom will be significant if condition (7) is fulfilled.

An investigation of channel stability with the use of probability theory showed that, as a stable canal section forms, a decrease of the probability of removal of particles in the edge zone to zero is characteristic. In this case the probability of removal of particles in the remaining part of the cross section is equal to unity, which corresponds to intense movement of sediments. Thus, an approach of the probability of removal of particles near the side boundary of the flow to zero can be regarded as a criterion of channel stability. Figure 8 (curve 3) shows the distribution of the probability of removal of particles  $\eta$  in the channel cross section at different stages of its formation (experiment 2). Noteworthy here is the different character of variation of  $\eta$  over the width of the flow in the initial and subsequent stages of channel formation. In the first case the value of  $\eta$  decreases from the water edge toward the middle of the flow. In the other two stages of channel formation shown in the figures (Fig. 5) the value of  $\eta$  increases from the water edge toward the middle of the flow.

The investigations showed that the acceptance of the mean velocity of the flow in a canal according to the "permissible velocity" method or the assignment of its parameters according to the "tractive force" method is not an index of the stability of the planned channel. The dynamic stability of a canal cross section should be calculated with consideration of not only the average but also of the fluctuation characteristics of the flow.

#### LITERATURE CITED

1. M. A. Velikanov, Dynamics of Channel Streams. Sediments and the Channel [in Russian], Vol. 2, Gostekhizdat, Moscow (1955).
2. V. T. Chow, Open-Channel Hydraulics, McGraw-Hill, New York (1959).
3. V. P. Petrov, "Apparatus, methods, and investigation of turbulent fluctuations of concentration and velocity in a sediment-transporting channel stream," Author's Abstract of Candidate's Dissertation, Moscow State Univ. (1971).



4. G. M. Jenkins and D. G. Watts, *Spectral Analysis and Its Applications*, Holden-Day, San Francisco (1968).